Selected for a Viewpoint in *Physics*

Observation of a Charged Charmoniumlike Structure in $e^+e^- \to \pi^+\pi^- J/\psi$ at $\sqrt{s} = 4.26$ GeV

M. Ablikim,[1] M. N. Achasov,[6] X. C. Ai,[1] O. Albayrak,[3] D. J. Ambrose,[39] F. F. An,[1] Q. An,[40] J.Z. Bai,[1]
R. Baldini Ferroli,[17a] Y. Ban,[26] J. Becker,[2] J. V. Bennett,[16] M. Bertani,[17a] J. M. Bian,[38] E. Boger,[19,*] O. Bondarenko,[20]
I. Boyko,[19] R. A. Briere,[3] V. Bytev,[19] H. Cai,[44] X. Cai,[1] O. Cakir,[34a] A. Calcaterra,[17a] G. F. Cao,[1] S. A. Cetin,[34b]
J. F. Chang,[1] G. Chelkov,[19,*] G. Chen,[1] H. S. Chen,[1] J. C. Chen,[1] M. L. Chen,[1] S. J. Chen,[24] X. Chen,[26] Y. B. Chen,[1]
H. P. Cheng,[14] Y. P. Chu,[1] D. Cronin-Hennessy,[38] H. L. Dai,[1] J. P. Dai,[1] D. Dedovich,[19] Z. Y. Deng,[1] A. Denig,[18]
I. Denysenko,[19,†] M. Destefanis,[43a,43c] W. M. Ding,[28] Y. Ding,[22] L. Y. Dong,[1] M. Y. Dong,[1] S. X. Du,[46] J. Fang,[1]
S. S. Fang,[1] L. Fava,[43b,43c] C. Q. Feng,[40] P. Friedel,[2] C. D. Fu,[1] J. L. Fu,[24] O. Fuks,[19,*] Q. Gao,[1] Y. Gao,[33] C. Geng,[40]
K. Goetzen,[7] W. X. Gong,[1] W. Gradl,[18] M. Greco,[43a,43c] M. H. Gu,[1] Y. T. Gu,[9] Y. H. Guan,[36] A. Q. Guo,[25] L. B. Guo,[23]
T. Guo,[23] Y. P. Guo,[25] Y. L. Han,[1] F. A. Harris,[37] K. L. He,[1] M. He,[1] Z. Y. He,[25] T. Held,[2] Y. K. Heng,[1] Z. L. Hou,[1] C. Hu,[23]
H. M. Hu,[1] J. F. Hu,[35] T. Hu,[1] G. M. Huang,[4] G. S. Huang,[40] J. S. Huang,[12] L. Huang,[1] X. T. Huang,[28] Y. Huang,[24]
Y. P. Huang,[1] T. Hussain,[42] C. S. Ji,[40] Q. Ji,[1] Q. P. Ji,[25] X. B. Ji,[1] X. L. Ji,[1] L. L. Jiang,[1] X. S. Jiang,[1] J. B. Jiao,[28] Z. Jiao,[14]
D. P. Jin,[1] S. Jin,[1] F. F. Jing,[33] N. Kalantar-Nayestanaki,[20] M. Kavatsyuk,[20] B. Kopf,[2] M. Kornicer,[37] W. Kühn,[35] W. Lai,[1]
J. S. Lange,[35] M. Lara,[16] P. Larin,[11] M. Leyhe,[2] C. H. Li,[1] Cheng Li,[40] Cui Li,[40] D. M. Li,[46] F. Li,[1] G. Li,[1] H. B. Li,[1]
J. C. Li,[1] K. Li,[10] Lei Li,[1] Q. J. Li,[1] S. L. Li,[1] W. D. Li,[1] W. G. Li,[1] X. L. Li,[28] X. N. Li,[1] X. Q. Li,[25] X. R. Li,[27] Z. B. Li,[32]
H. Liang,[40] Y. F. Liang,[30] Y. T. Liang,[35] G. R. Liao,[33] X. T. Liao,[1] D. Lin,[11] B. J. Liu,[1] C. L. Liu,[3] C. X. Liu,[1] F. H. Liu,[29]
Fang Liu,[1] Feng Liu,[4] H. Liu,[1] H. B. Liu,[9] H. H. Liu,[13] H. M. Liu,[1] H. W. Liu,[1] J. P. Liu,[44] K. Liu,[33] K. Y. Liu,[22] Kai Liu,[36]
P. L. Liu,[28] Q. Liu,[36] S. B. Liu,[40] X. Liu,[21] Y. B. Liu,[25] Z. A. Liu,[1] Zhiqiang Liu,[1] Zhiqing Liu,[1] H. Loehner,[20] X. C. Lou,[1,‡]
G. R. Lu,[12] H. J. Lu,[14] J. G. Lu,[1] Q. W. Lu,[29] X. R. Lu,[36] Y. P. Lu,[1] C. L. Luo,[23] M. X. Luo,[45] T. Luo,[37] X. L. Luo,[1] M. Lv,[1]
C. L. Ma,[36] F. C. Ma,[22] H. L. Ma,[1] Q. M. Ma,[1] S. Ma,[1] T. Ma,[1] X. Y. Ma,[1] F. E. Maas,[11] M. Maggiora,[43a,43c] Q. A. Malik,[42]
Y. J. Mao,[26] Z. P. Mao,[1] J. G. Messchendorp,[20] J. Min,[1] T. J. Min,[1] R. E. Mitchell,[16] X. H. Mo,[1] Y. J. Mo,[10] H. Moeini,[20]
C. Morales Morales,[11] K. Moriya,[16] N. Yu. Muchnoi,[6] H. Muramatsu,[39] Y. Nefedov,[19] C. Nicholson,[36] I. B. Nikolaev,[6]
Z. Ning,[1] S. L. Olsen,[27] Q. Ouyang,[1] S. Pacetti,[17b] J. W. Park,[27] M. Pelizaeus,[2] H. P. Peng,[40] K. Peters,[7] J. L. Ping,[23]
R. G. Ping,[1] R. Poling,[38] E. Prencipe,[18] M. Qi,[24] S. Qian,[1] C. F. Qiao,[36] L. Q. Qin,[28] X. S. Qin,[1] Y. Qin,[26] Z. H. Qin,[1]
J. F. Qiu,[1] K. H. Rashid,[42] G. Rong,[1] X. D. Ruan,[9] A. Sarantsev,[19,§] B. D. Schaefer,[16] M. Shao,[40] C. P. Shen,[37,‖] X. Y. Shen,[1]
H. Y. Sheng,[1] M. R. Shepherd,[16] W. M. Song,[1] X. Y. Song,[1] S. Spataro,[43a,43c] B. Spruck,[35] D. H. Sun,[1] G. X. Sun,[1]
J. F. Sun,[12] S. S. Sun,[1] Y. J. Sun,[40] Y. Z. Sun,[1] Z. J. Sun,[1] Z. T. Sun,[40] C. J. Tang,[30] X. Tang,[1] I. Tapan,[34c] E. H. Thorndike,[39]
D. Toth,[38] M. Ullrich,[35] I. Uman,[34b] G. S. Varner,[37] B. Q. Wang,[26] D. Wang,[26] D. Y. Wang,[26] K. Wang,[1] L. L. Wang,[1]
L. S. Wang,[1] M. Wang,[28] P. Wang,[1] P. L. Wang,[1] Q. J. Wang,[1] S. G. Wang,[26] X. F. Wang,[33] X. L. Wang,[40] Y. D. Wang,[17a]
Y. F. Wang,[1] Y. Q. Wang,[18] Z. Wang,[1] Z. G. Wang,[1] Z. Y. Wang,[1] D. H. Wei,[8] J. B. Wei,[26] P. Weidenkaff,[18] Q. G. Wen,[40]
S. P. Wen,[1] M. Werner,[35] U. Wiedner,[2] L. H. Wu,[1] N. Wu,[1] S. X. Wu,[40] W. Wu,[25] Z. Wu,[1] L. G. Xia,[33] Y. X. Xia,[15]
Z. J. Xiao,[23] Y. G. Xie,[1] Q. L. Xiu,[1] G. F. Xu,[1] G. M. Xu,[26] Q. J. Xu,[10] Q. N. Xu,[36] X. P. Xu,[31] Z. R. Xu,[40] F. Xue,[4] Z. Xue,[1]
L. Yan,[40] W. B. Yan,[40] Y. H. Yan,[15] H. X. Yang,[1] Y. Yang,[4] Y. X. Yang,[8] H. Ye,[1] M. Ye,[1] M. H. Ye,[5] B. X. Yu,[1] C. X. Yu,[25]
H. W. Yu,[26] J. S. Yu,[21] S. P. Yu,[28] C. Z. Yuan,[1] Y. Yuan,[1] A. A. Zafar,[42] A. Zallo,[17a] S. L. Zang,[24] Y. Zeng,[15] B. X. Zhang,[1]
B. Y. Zhang,[1] C. Zhang,[24] C. C. Zhang,[1] D. H. Zhang,[1] H. H. Zhang,[32] H. Y. Zhang,[1] J. Q. Zhang,[1] J. W. Zhang,[1]
J. Y. Zhang,[1] J. Z. Zhang,[1] LiLi Zhang,[15] R. Zhang,[36] S. H. Zhang,[1] X. J. Zhang,[1] X. Y. Zhang,[28] Y. Zhang,[1] Y. H. Zhang,[1]
Z. P. Zhang,[40] Z. Y. Zhang,[44] Zhenghao Zhang,[4] G. Zhao,[1] H. S. Zhao,[1] J. W. Zhao,[1] K. X. Zhao,[23] Lei Zhao,[40] Ling Zhao,[1]
M. G. Zhao,[25] Q. Zhao,[1] S. J. Zhao,[46] T. C. Zhao,[1] X. H. Zhao,[24] Y. B. Zhao,[1] Z. G. Zhao,[40] A. Zhemchugov,[19,*]
B. Zheng,[41] J. P. Zheng,[1] Y. H. Zheng,[36] B. Zhong,[23] L. Zhou,[1] X. Zhou,[44] X. K. Zhou,[36] X. R. Zhou,[40] C. Zhu,[1] K. Zhu,[1]
K. J. Zhu,[1] S. H. Zhu,[1] X. L. Zhu,[33] Y. C. Zhu,[40] Y. M. Zhu,[25] Y. S. Zhu,[1] Z. A. Zhu,[1] J. Zhuang,[1] B. S. Zou,[1] and J. H. Zou[1]

(BESIII Collaboration)

[1]*Institute of High Energy Physics, Beijing 100049, People's Republic of China*
[2]*Bochum Ruhr-University, D-44780 Bochum, Germany*
[3]*Carnegie Mellon University, Pittsburgh, Pennsylvania 15213, USA*
[4]*Central China Normal University, Wuhan 430079, People's Republic of China*
[5]*China Center of Advanced Science and Technology, Beijing 100190, People's Republic of China*
[6]*G. I. Budker Institute of Nuclear Physics SB RAS (BINP), Novosibirsk 630090, Russia*
[7]*GSI Helmholtzcentre for Heavy Ion Research GmbH, D-64291 Darmstadt, Germany*
[8]*Guangxi Normal University, Guilin 541004, People's Republic of China*

[9]GuangXi University, Nanning 530004, People's Republic of China

[10]Hangzhou Normal University, Hangzhou 310036, People's Republic of China

[11]Helmholtz Institute Mainz, Johann-Joachim-Becher-Weg 45, D-55099 Mainz, Germany

[12]Henan Normal University, Xinxiang 453007, People's Republic of China

[13]Henan University of Science and Technology, Luoyang 471003, People's Republic of China

[14]Huangshan College, Huangshan 245000, People's Republic of China

[15]Hunan University, Changsha 410082, People's Republic of China

[16]Indiana University, Bloomington, Indiana 47405, USA

[17a]INFN Laboratori Nazionali di Frascati, I-00044 Frascati, Italy

[17b]INFN and University of Perugia, I-06100 Perugia, Italy

[18]Johannes Gutenberg University of Mainz, Johann-Joachim-Becher-Weg 45, D-55099 Mainz, Germany

[19]Joint Institute for Nuclear Research, 141980 Dubna, Moscow region, Russia

[20]KVI, University of Groningen, NL-9747 AA Groningen, The Netherlands

[21]Lanzhou University, Lanzhou 730000, People's Republic of China

[22]Liaoning University, Shenyang 110036, People's Republic of China

[23]Nanjing Normal University, Nanjing 210023, People's Republic of China

[24]Nanjing University, Nanjing 210093, People's Republic of China

[25]Nankai University, Tianjin 300071, People's Republic of China

[26]Peking University, Beijing 100871, People's Republic of China

[27]Seoul National University, Seoul 151-747 Korea

[28]Shandong University, Jinan 250100, People's Republic of China

[29]Shanxi University, Taiyuan 030006, People's Republic of China

[30]Sichuan University, Chengdu 610064, People's Republic of China

[31]Soochow University, Suzhou 215006, People's Republic of China

[32]Sun Yat-Sen University, Guangzhou 510275, People's Republic of China

[33]Tsinghua University, Beijing 100084, People's Republic of China

[34a]Ankara University, Dogol Caddesi, 06100 Tandogan, Ankara, Turkey

[34b]Dogus University, 34722 Istanbul, Turkey

[34c]Uludag University, 16059 Bursa, Turkey

[35]Universität Giessen, D-35392 Giessen, Germany

[36]University of Chinese Academy of Sciences, Beijing 100049, People's Republic of China

[37]University of Hawaii, Honolulu, Hawaii 96822, USA

[38]University of Minnesota, Minneapolis, Minnesota 55455, USA

[39]University of Rochester, Rochester, New York 14627, USA

[40]University of Science and Technology of China, Hefei 230026, People's Republic of China

[41]University of South China, Hengyang 421001, People's Republic of China

[42]University of the Punjab, Lahore 54590, Pakistan

[43a]University of Turin, I-10125 Turin, Italy

[43b]University of Eastern Piedmont, I-15121 Alessandria, Italy

[43c]INFN, I-10125 Turin, Italy

[44]Wuhan University, Wuhan 430072, People's Republic of China

[45]Zhejiang University, Hangzhou 310027, People's Republic of China

[46]Zhengzhou University, Zhengzhou 450001, People's Republic of China

We study the process $e^+e^- \to \pi^+\pi^- J/\psi$ at a center-of-mass energy of 4.260 GeV using a 525 pb^{-1} data sample collected with the BESIII detector operating at the Beijing Electron Positron Collider. The Born cross section is measured to be $(62.9 \pm 1.9 \pm 3.7)$ pb, consistent with the production of the $Y(4260)$. We observe a structure at around 3.9 GeV/c^2 in the $\pi^\pm J/\psi$ mass spectrum, which we refer to as the $Z_c(3900)$. If interpreted as a new particle, it is unusual in that it carries an electric charge and couples to charmonium. A fit to the $\pi^\pm J/\psi$ invariant mass spectrum, neglecting interference, results in a mass of $(3899.0 \pm 3.6 \pm 4.9)$ MeV/c^2 and a width of $(46 \pm 10 \pm 20)$ MeV. Its production ratio is measured to be $R = (\sigma(e^+e^- \to \pi^\pm Z_c(3900)^\mp \to \pi^+\pi^- J/\psi)/\sigma(e^+e^- \to \pi^+\pi^- J/\psi)) = (21.5 \pm 3.3 \pm 7.5)\%$. In all measurements the first errors are statistical and the second are systematic.

Since its discovery in the initial-state-radiation (ISR) process $e^+e^- \to \gamma_{\mathrm{ISR}} \pi^+\pi^- J/\psi$ [1], and despite its subsequent observations [2–5], the nature of the $Y(4260)$ state has remained a mystery. Unlike other charmonium states with the same quantum numbers and in the same mass region, such as the $\psi(4040)$, $\psi(4160)$, and $\psi(4415)$, the

$Y(4260)$ state does not have a natural place within the quark model of charmonium [6]. Furthermore, while being well above the $D\bar{D}$ threshold, the $Y(4260)$ shows strong coupling to the $\pi^+\pi^- J/\psi$ final state [7], but relatively small coupling to open charm decay modes [8–12]. These properties perhaps indicate that the $Y(4260)$ state is not a conventional state of charmonium [13].

A similar situation has recently become apparent in the bottomonium system above the $B\bar{B}$ threshold, where there are indications of anomalously large couplings between the $\Upsilon(5S)$ state [or perhaps an unconventional bottomonium state with similar mass, the $Y_b(10890)$] and the $\pi^+\pi^- \Upsilon(1S, 2S, 3S)$ and $\pi^+\pi^- h_b(1P, 2P)$ final states [14,15]. More surprisingly, substructure in these $\pi^+\pi^- \Upsilon(1S, 2S, 3S)$ and $\pi^+\pi^- h_b(1P, 2P)$ decays indicates the possible existence of charged bottomoniumlike states [16], which must have at least four constituent quarks to have a nonzero electric charge, rather than the two in a conventional meson. By analogy, this suggests there may exist interesting substructure in the $Y(4260) \rightarrow \pi^+\pi^- J/\psi$ process in the charmonium region.

In this Letter, we present a study of the process $e^+e^- \rightarrow \pi^+\pi^- J/\psi$ at a center-of-mass (c.m.) energy of $\sqrt{s} = (4.260 \pm 0.001)$ GeV, which corresponds to the peak of the $Y(4260)$ cross section. We observe a charged structure in the $\pi^\pm J/\psi$ invariant mass spectrum, which we refer to as the $Z_c(3900)$. The analysis is performed with a 525 pb^{-1} data sample collected with the BESIII detector, which is described in detail in Ref. [17]. In the studies presented here, we rely only on charged particle tracking in the main drift chamber and energy deposition in the electromagnetic calorimeter (EMC).

The GEANT4-based Monte Carlo (MC) simulation software, which includes the geometric description of the BESIII detector and the detector response, is used to optimize the event selection criteria, determine the detection efficiency, and estimate backgrounds. For the signal process, we use a sample of $e^+e^- \rightarrow \pi^+\pi^- J/\psi$ MC events generated assuming the $\pi^+\pi^- J/\psi$ is produced via $Y(4260)$ decays, and using the $e^+e^- \rightarrow \pi^+\pi^- J/\psi$ cross sections measured by Belle [3] and *BABAR* [5]. The $\pi^+\pi^- J/\psi$ substructure is modelled according to the

experimentally observed Dalitz plot distribution presented in this analysis. ISR is simulated with KKMC [18] with a maximum energy of 435 MeV for the ISR photon, corresponding to a $\pi^+\pi^- J/\psi$ mass of 3.8 GeV/c^2.

For $e^+e^- \rightarrow \pi^+\pi^- J/\psi$ events, the J/ψ candidate is reconstructed with lepton pairs (e^+e^- or $\mu^+\mu^-$). Since this decay results in a final state with four charged particles, we first select events with four good charged tracks with net charge zero. For each charged track, the polar angle in the main drift chamber must satisfy $|\cos\theta| < 0.93$, and the point of closest approach to the e^+e^- interaction point must be within ± 10 cm in the beam direction and within 1 cm in the plane perpendicular to the beam direction. Since pions and leptons are kinematically well separated in this decay, charged tracks with momenta larger than 1.0 GeV/c in the lab frame are assumed to be leptons, and the others are assumed to be pions. We use the energy deposited in the EMC to separate electrons from muons. For muon candidates, the deposited energy in the EMC should be less than 0.35 GeV, while for electrons, it should be larger than 1.1 GeV. The efficiencies of these requirements are determined from MC simulation to be above 99% in the EMC sensitive region.

In order to reject radiative Bhabha and radiative dimuon ($\gamma e^+e^-/\gamma\mu^+\mu^-$) backgrounds associated with a photon-conversion, the cosine of the opening angle of the pion candidates, which are true e^+e^- pairs in the case of background, is required to be less than 0.98. In the e^+e^- mode, the same requirement is imposed on the $\pi^\pm e^\mp$ opening angles. This restriction removes less than 1% of the signal events.

The lepton pair and the two pions are subjected to a four-constraint (4C) kinematic fit to the total initial four-momentum of the colliding beams in order to improve the momentum resolution and reduce the background. The χ^2 of the kinematic fit is required to be less than 60.

After imposing these selection criteria, the invariant mass distributions of the lepton pairs are shown in Fig. 1. A clear J/ψ signal is observed in both the e^+e^- and $\mu^+\mu^-$ modes. There are still remaining $e^+e^- \rightarrow \pi^+\pi^- \pi^+\pi^-$, and other QED backgrounds, but these can be estimated using the events in the J/ψ mass sideband.
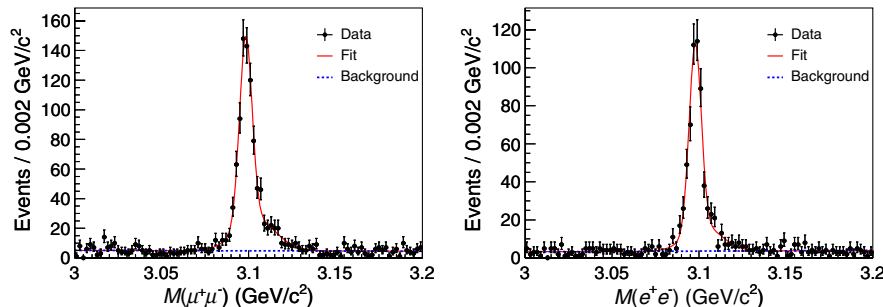

FIG. 1 (color online). The distributions of $M(\mu^+\mu^-)$ (left panel) and $M(e^+e^-)$ (right panel) after performing a 4C kinematic fit and imposing all selection criteria. Dots with error bars are data and the curves are the best fit described in the text.

The final selection efficiency is $(53.8 \pm 0.3)\%$ for $\mu^+\mu^-$ events and $(38.4 \pm 0.3)\%$ for e^+e^- events, where the errors are from the statistics of the MC sample. The main factors affecting the detection efficiencies include the detector acceptances for four charged tracks and the requirement on the quality of the kinematic fit adopted. The lower efficiency for e^+e^- events is due to final-state-radiation, bremsstrahlung energy loss of e^+e^- pairs, and the EMC deposit energy requirement.

To extract the number of $\pi^+\pi^- J/\psi$ signal events, invariant mass distributions of the lepton pairs are fit using the sum of two Gaussian functions with a linear background term. The fits yield $M(J/\psi) = (3098.4 \pm 0.2)$ MeV/c^2 with 882 ± 33 signal events in the $\mu^+\mu^-$ mode, and $M(J/\psi) = (3097.9 \pm 0.3)$ MeV/c^2 with 595 ± 28 signal events in the e^+e^- mode. Here the errors are statistical only. The mass resolution is 3.7 MeV/c^2 in the $\mu^+\mu^-$ mode and 4.0 MeV/c^2 in the e^+e^- mode.

The Born cross section is determined from the relation $\sigma^B = (N^{\text{fit}}/\mathcal{L}_{\text{int}}(1+\delta)\epsilon\mathcal{B})$, where N^{fit} is the number of signal events from the fit; $\mathcal{L}_{\text{int}}$ is the integrated luminosity, ϵ is the selection efficiency obtained from a MC simulation, $\mathcal{B}$ is the branching fraction of $J/\psi \to \ell^+\ell^-$, and $(1+\delta)$ is the radiative correction factor, which is 0.818 according to a QED calculation [19]. The measured Born cross section for $e^+e^- \to \pi^+\pi^- J/\psi$ is (64.4 ± 2.4) pb in the $\mu^+\mu^-$ mode and (60.7 ± 2.9) pb in the e^+e^- mode. The combined measurement is $\sigma^B(e^+e^- \to \pi^+\pi^- J/\psi) = (62.9 \pm 1.9)$ pb.

Systematic errors in the cross section measurement come from the luminosity measurement, tracking efficiency, kinematic fit, background estimation, dilepton branching fractions of the J/ψ, and $Y(4260)$ decay dynamics.

The integrated luminosity of this data sample was measured using large angle Bhabha events, and has an estimated uncertainty of 1.0%. The tracking efficiency uncertainty is estimated to be 1% for each track from a study of the control samples $J/\psi \to \pi^+\pi^-\pi^0$ and $\psi(3686) \to \pi^+\pi^- J/\psi$. Since the luminosity is measured using Bhabha events, the tracking efficiency uncertainty of high momentum lepton pairs partly cancels in the calculation of the $\pi^+\pi^- J/\psi$ cross section. To be conservative, we take 4% for both the e^+e^- and $\mu^+\mu^-$ modes.

The uncertainty from the kinematic fit comes from the inconsistency between the data and MC simulation of the track helix parameters. Following the procedure described in Ref. [20], we take the difference between the efficiencies with and without the helix parameter correction as the systematic error, which is 2.2% in the $\mu^+\mu^-$ mode and 2.3% in the e^+e^- mode.

Uncertainties due to the choice of background shape and fit range are estimated by varying the background function from linear to a second-order polynomial and by extending the fit range.

Uncertainties in the $Y(4260)$ resonance parameters and possible distortions of the $Y(4260)$ line shape introduce small systematic uncertainties in the radiative correction factor and the efficiency. This is estimated using the different line shapes measured by Belle [3] and BABAR [5]. The difference in $(1+\delta)\epsilon$ is 0.6% in both the e^+e^- and $\mu^+\mu^-$ modes, and this is taken as a systematic error.

We use the observed Dalitz plot to generate $Y(4260) \to \pi^+\pi^- J/\psi$ events. To cover possible modelling inaccuracies, we conservatively take the difference between the efficiency using this model and the efficiency using a phase space model as a systematic error. The error is 3.1% in both the $\mu^+\mu^-$ and the e^+e^- modes.

The uncertainty in $\mathcal{B}(J/\psi \to \ell^+\ell^-)$ is 1% [21]. The trigger simulation, the event start time determination, and the final-state-radiation simulation are well understood; the total systematic error due to these sources is estimated to be less than 1%.

Assuming all of the sources are independent, the total systematic error in the $\pi^+\pi^- J/\psi$ cross section measurement is determined to be 5.9% for the $\mu^+\mu^-$ mode and 6.8% for the e^+e^- mode. Taking the correlations in errors between the two modes into account, the combined systematic error is slightly less than 5.9%.

Intermediate states are studied by examining the Dalitz plot of the selected $\pi^+\pi^- J/\psi$ candidate events. The J/ψ signal is selected using $3.08 < M(\ell^+\ell^-) < 3.12$ GeV/c^2 and the sideband using $3.00 < M(\ell^+\ell^-) < 3.06$ GeV/c^2 or $3.14 < M(\ell^+\ell^-) < 3.20$ GeV/c^2, which is three times the size of the signal region. In total, a sample of 1595 $\pi^+\pi^- J/\psi$ events with a purity of 90% is obtained.

Figure 2 shows the Dalitz plot of events in the J/ψ signal region, where there are structures in the $\pi^+\pi^-$ system and evidence for an exotic charmoniumlike structure in the $\pi^\pm J/\psi$ system. The inset shows background events from J/ψ mass sidebands (not normalized), where no obvious structures are observed.
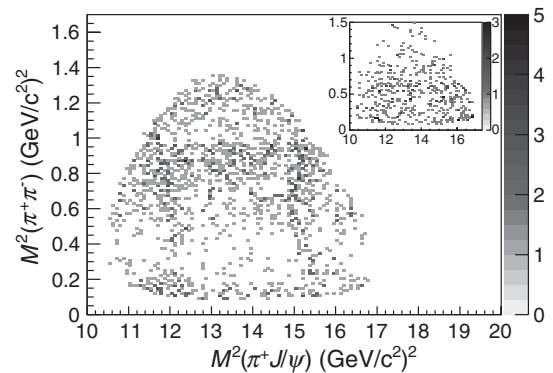

FIG. 2. Dalitz distributions of $M^2(\pi^+\pi^-)$ vs $M^2(\pi^+ J/\psi)$ for selected $e^+e^- \to \pi^+\pi^- J/\psi$ events in the J/ψ signal region. The inset shows background events from the J/ψ mass sidebands (not normalized).

Figure 3 shows the projections of the $M(\pi^+ J/\psi)$, $M(\pi^- J/\psi)$, and $M(\pi^+\pi^-)$ distributions for the signal events, as well as the background events estimated from normalized J/ψ mass sidebands. In the $\pi^\pm J/\psi$ mass spectrum, there is a significant peak at around 3.9 GeV/c^2 [referred to as the $Z_c(3900)$ hereafter]. The wider peak at low mass is a reflection of the $Z_c(3900)$ as indicated from MC simulation, and shown in Fig. 3. Similar structures are observed in the e^+e^- and $\mu^+\mu^-$ separated samples.

The $\pi^+\pi^-$ mass spectrum shows nontrivial structure. To test the possible effects of dynamics in the $\pi^+\pi^-$ mass spectrum on the $\pi^\pm J/\psi$ projection, we develop a parametrization for the $\pi^+\pi^-$ mass spectrum that includes a $f_0(980)$, $\sigma(500)$, and a nonresonant amplitude. An MC sample generated with this parametrization adequately describes the $\pi^+\pi^-$ spectrum, as shown in Fig. 3, but does not generate any peaking structure in the $\pi^\pm J/\psi$ projection consistent with the $Z_c(3900)$. We have also tested D-wave $\pi^+\pi^-$ amplitudes, which are not apparent in the data, and they, also, do not generate peaks in the $\pi^\pm J/\psi$ spectrum.

An unbinned maximum likelihood fit is applied to the distribution of $M_{\max}(\pi^\pm J/\psi)$, the larger one of the two mass combinations $M(\pi^+ J/\psi)$ and $M(\pi^- J/\psi)$ in each event. The signal shape is parametrized as an S-wave Breit-Wigner function convolved with a Gaussian with a mass resolution fixed at the MC simulated value (4.2 MeV/c^2). The phase space factor $p \cdot q$ is considered in the partial width, where p is the $Z_c(3900)$ momentum in the $Y(4260)$ c.m. frame and q is the J/ψ momentum in the $Z_c(3900)$ c.m. frame. The background shape is parametrized as $a/(x - 3.6)^b + c + dx$, where a, b, c, and d are free parameters and $x = M_{\max}(\pi^\pm J/\psi)$. The efficiency curve is considered in the fit and the possible interference between the signal and background is neglected. Figure 4 shows the fit results; the fit yields a mass of (3899.0 ± 3.6) MeV/c^2, and a width of (46 ± 10) MeV. The goodness of the fit is found to be $\chi^2/\text{ndf} = 32.6/37 = 0.9$.

The number of $Z_c(3900)$ events is determined to be $N[Z_c(3900)^\pm] = 307 \pm 48$. The production ratio is calculated to be $R = \sigma(e^+e^- \to \pi^\pm Z_c(3900)^\mp \to \pi^+\pi^- J/\psi)/\sigma(e^+e^- \to \pi^+\pi^- J/\psi) = (21.5 \pm 3.3)\%$, where the efficiency correction has been applied. The statistical significance is calculated by comparing the fit likelihoods with and without the signal. Besides the nominal fit, the fit is also performed by changing the fit range, the signal shape, or the background shape. In all cases, the significance is found to be greater than 8σ.

Fitting the $M(\pi^+ J/\psi)$ and $M(\pi^- J/\psi)$ distributions separately, one obtains masses, widths, and production rates of the $Z_c(3900)^+$ and $Z_c(3900)^-$ that agree with each other within statistical errors. Dividing the sample into two different $M(\pi^+\pi^-)$ regions [below and above $M^2(\pi^+\pi^-) = 0.7$ GeV$^2/c^4$] allows us to check the robustness of the $Z_c(3900)$ signal in the presence of two different sets of interfering $\pi^+\pi^- J/\psi$ amplitudes. In both samples, the $Z_c(3900)$ is significant and the observed mass can shift by as much as 14 ± 5 MeV/c^2 from the nominal fit, and the width can shift by (20 ± 11) MeV. We attribute the systematic shifts in mass and width to interference between the $Z_c(3900)\pi$ and $(\pi^+\pi^-)J/\psi$ amplitudes. In fitting the $\pi^\pm J/\psi$ projection of the Dalitz plot, our analysis averages over the entire $\pi^+\pi^-$ spectrum, and our measurement of the $Z_c(3900)$ mass, width, and production fraction neglects interference with other $\pi^+\pi^- J/\psi$ amplitudes.

The systematic errors for the resonance parameters of the $Z_c(3900)$ come from the mass calibration, parametrization of the signal and background shapes, and the mass resolution. The uncertainty from the mass calibration can be estimated using the difference between the measured and known J/ψ masses (reconstructed from e^+e^- and $\mu^+\mu^-$) and D^0 masses (reconstructed from $K^-\pi^+$). The differences are (1.4 ± 0.2) MeV/c^2 and $-(0.7 \pm 0.2)$ MeV/c^2, respectively. Since our signal topology has one low momentum pion, as in D^0 decay, and a pair of high momentum tracks from the J/ψ decay, we assume these differences added in quadrature is the systematic error of the $Z_c(3900)$ mass measurement due to tracking. Doing a fit by assuming a P wave between the $Z_c(3900)$ and the π, and between the J/ψ and π in the $Z_c(3900)$ system, yields
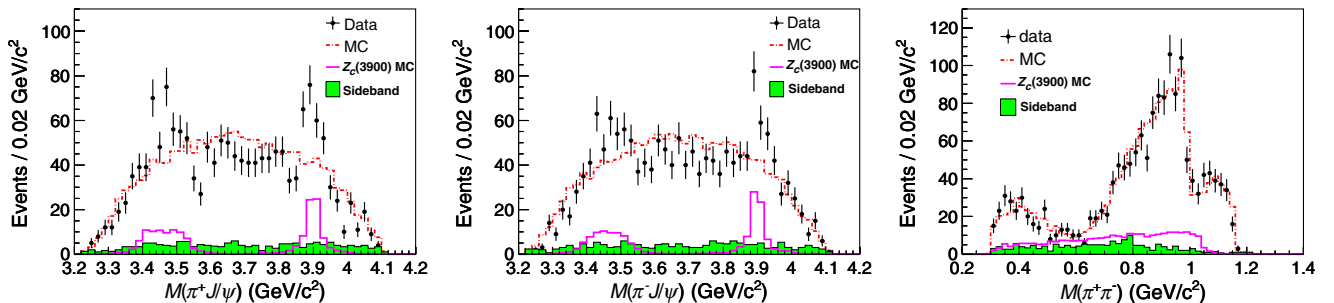

FIG. 3 (color online).   One dimensional projections of the $M(\pi^+ J/\psi)$, $M(\pi^- J/\psi)$, and $M(\pi^+\pi^-)$ invariant mass distributions in $e^+e^- \to \pi^+\pi^- J/\psi$ for data in the J/ψ signal region (dots with error bars), data in the J/ψ sideband region (shaded histograms), and MC simulation results from $\sigma(500)$, $f_0(980)$, and nonresonant $\pi^+\pi^-$ amplitudes (red dotted-dashed histograms). The pink blank histograms show a MC simulation of the $Z_c(3900)$ signal with arbitrary normalization.
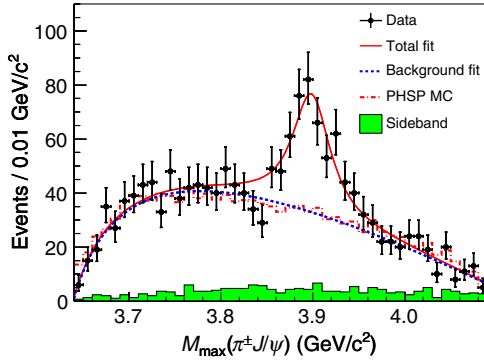
FIG. 4 (color online). Fit to the $M_{max}(\pi^{\pm}J/\psi)$ distribution as described in the text. Dots with error bars are data; the red solid curve shows the total fit, and the blue dotted curve the background from the fit; the red dotted-dashed histogram shows the result of a phase space (PHSP) MC simulation; and the green shaded histogram shows the normalized J/ψ sideband events.

a mass difference of 2.1 MeV/c^2, a width difference of 3.7 MeV, and production ratio difference of 2.6% absolute. Assuming the $Z_c(3900)$ couples strongly with $D\bar{D}^*$ results in an energy dependence of the total width [22], and the fit yields a difference of 2.1 MeV/c^2 for mass, 15.4 MeV for width, and no change for the production ratio. We estimate the uncertainty due to the background shape by changing to a third-order polynomial or a phase space shape, varying the fit range, and varying the requirements on the χ^2 of the kinematic fit. We find differences of 3.5 MeV/c^2 for mass, 12.1 MeV for width, and 7.1% absolute for the production ratio. Uncertainties due to the mass resolution are estimated by increasing the resolution determined by MC simulations by 16%, which is the difference between the MC simulated and measured mass resolutions of the J/ψ and D^0 signals. We find the difference is 1.0 MeV in the width, and 0.2% absolute in the production ratio, which are taken as the systematic errors. Assuming all the sources of systematic uncertainty are independent, the total systematic error is 4.9 MeV/c^2 for mass, 20 MeV for width and 7.5% for the production ratio.

In Summary, we have studied $e^+e^- \rightarrow \pi^+\pi^- J/\psi$ at a c.m. energy of 4.26 GeV. The cross section is measured to be $(62.9 \pm 1.9 \pm 3.7)$ pb, which agrees with the existing results from the *BABAR* [5], Belle [3], and CLEO [4] experiments. In addition, a structure with a mass of $(3899.0 \pm 3.6 \pm 4.9)$ MeV/c^2 and a width of $(46 \pm 10 \pm 20)$ MeV is observed in the $\pi^{\pm}J/\psi$ mass spectrum. This structure couples to charmonium and has an electric charge, which is suggestive of a state containing more quarks than just a charm and anticharm quark. Similar studies were performed in *B* decays, with unconfirmed structures reported in the $\pi^{\pm}\psi(3686)$ and $\pi^{\pm}\chi_{c1}$ systems [23–26]. It is also noted that model-dependent calculations exist that attempt to explain the charged bottomonium-like structures which may also apply to the charmonium-like structures, and there were model predictions of

charmoniumlike structures near the $D\bar{D}^*$ and $D^*\bar{D}^*$ thresholds [27].

*Also at the Moscow Institute of Physics and Technology, Moscow 141700, Russia.
†On leave from the Bogolyubov Institute for Theoretical Physics, Kiev 03680, Ukraine.
‡Also at University of Texas at Dallas, Richardson, Texas 75083, USA.
§Also at the PNPI, Gatchina 188300, Russia.
‖Present address: Nagoya University, Nagoya 464-8601, Japan.

[1] B. Aubert *et al.* (*BABAR* Collaboration), Phys. Rev. Lett. **95**, 142001 (2005).
[2] Q. He *et al.* (CLEO Collaboration), Phys. Rev. D **74**, 091104(R) (2006).
[3] C. Z. Yuan *et al.* (Belle Collaboration), Phys. Rev. Lett. **99**, 182004 (2007).
[4] T. E. Coan *et al.* (CLEO Collaboration), Phys. Rev. Lett. **96**, 162003 (2006).
[5] J. P. Lees *et al.* (*BABAR* Collaboration), Phys. Rev. D **86**, 051102(R) (2012).
[6] T. Barnes, S. Godfrey, and E. S. Swanson, Phys. Rev. D **72**, 054026 (2005).
[7] X. H. Mo, G. Li, C. Z. Yuan, K. L. He, H. M. Hu, J. H. Hu, P. Wang, and Z. Y. Wang, Phys. Lett. B **640**, 182 (2006).
[8] D. Cronin-Hennessy *et al.* (CLEO Collaboration), Phys. Rev. D **80**, 072001 (2009).
[9] G. Pakhlova *et al.* (Belle Collaboration), Phys. Rev. Lett. **98**, 092001 (2007).

[10] B. Aubert *et al.* (*BABAR* Collaboration), Phys. Rev. D **76,** 111105 (2007).

[11] B. Aubert *et al.* (*BABAR* Collaboration), Phys. Rev. D **79,** 092001 (2009).

[12] P. del Amo Sanchez *et al.* (*BABAR* Collaboration), Phys. Rev. D **82,** 052004 (2010).

[13] For a recent review, see N. Brambilla *et al.*, Eur. Phys. J. C **71,** 1 (2011).

[14] K.-F Chen *et al.* (Belle Collaboration), Phys. Rev. Lett. **100,** 112001 (2008).

[15] I. Adachi *et al.* (Belle Collaboration), Phys. Rev. Lett. **108,** 032001 (2012).

[16] A. Bondar *et al.* (Belle Collaboration), Phys. Rev. Lett. **108,** 122001 (2012).

[17] M. Ablikim *et al.* (BESIII Collaboration), Nucl. Instrum. Methods Phys. Res., Sect. A **614,** 345 (2010).

[18] S. Jadach, B. F. L. Ward, and Z. Was, Comput. Phys. Commun. **130,** 260 (2000); Phys. Rev. D **63,** 113009 (2001).

[19] E. A. Kuraev and V. S. Fadin, Yad. Fiz. **41,** 733 (1985) [Sov. J. Nucl. Phys. **41,** 466 (1985)].

[20] M. Ablikim *et al.* (BESIII Collaboration), Phys. Rev. D **87,** 012002 (2013).

[21] J. Beringer *et al.* (Particle Data Group), Phys. Rev. D **86,** 010001 (2012).

[22] S. Flatté, Phys. Lett. **63B,** 224 (1976).

[23] S. K. Choi *et al.* (Belle Collaboration), Phys. Rev. Lett. **100,** 142001 (2008).

[24] B. Aubert *et al.* (*BABAR* Collaboration), Phys. Rev. D **79,** 112001 (2009).

[25] R. Mizuk *et al.* (Belle Collaboration), Phys. Rev. D **78,** 072004 (2008).

[26] J. P. Lees *et al.* (*BABAR* Collaboration), Phys. Rev. D **85,** 052003 (2012).

[27] L. Maiani, F. Piccinini, A. D. Polosa, and V. Riquer, Phys. Rev. D **71,** 014028 (2005); D.-Y. Chen, X. Liu, and T. Matsuki, arXiv:1208.2411; D.-Y. Chen and X. Liu, Phys. Rev. D **84,** 034032 (2011); Z.-F. Sun, J. He, X. Liu, Z.-G. Luo, and S.-L. Zhu, Phys. Rev. D **84,** 054002 (2011); Chinese Phys. C **36,** 194 (2012); A. Ali, C. Hambrock, and W. Wang, Phys. Rev. D **85,** 054011 (2012).